Properties of a Model of Ca^{++}-Dependent Vesicle Pool Dynamics and Short Term Synaptic Depression

Sibylle Weis, Ralf Schneggenburger, and Erwin Neher
Abt. Membranbiophysik, Max-Planck-Institut für biophysikalische Chemie, Am Fassberg 11, D-37077 Göttingen, Germany

ABSTRACT We explore the properties of models of synaptic vesicle dynamics, in which synaptic depression is attributed to depletion of a pool of release-ready vesicles. Two alternative formulations of the model allow for either recruitment of vesicles from an unlimited reserve pool (vesicle state model) or for recovery of a fixed number of release sites to a release-ready state (release-site model). It is assumed that, following transmitter release, the recovery of the release-ready pool of vesicles is regulated by the intracellular free Ca^{++} concentration, $[Ca^{++}]_i$. Considering the kinetics of $[Ca^{++}]_i$ after single presynaptic action potentials, we show that pool recovery can be described by two distinct kinetic components. With such a model, complex kinetic and steady-state properties of synaptic depression as found in several types of synapses can be accurately described. However, the specific assumption that enhanced recovery is proportional to $[Ca^{++}]_i$, as measured with Ca^{++} indicator dyes, is not confirmed by experiments at the calyx of Held, in which $[Ca^{++}]_i$-homeostasis was altered by adding low concentrations of the exogenous Ca^{++} buffer, fura-2, to the presynaptic terminal. We conclude that synaptic depression at the calyx of Held is governed by localized, near membrane $[Ca^{++}]_i$ signals not visible to the indicator dye, or else by an altogether different mechanism. We demonstrate that, in models in which a Ca^{++}-dependent process is linearly related to $[Ca^{++}]_i$, the addition of buffers has only transient but not steady-state consequences.

INTRODUCTION

Depletion of a pool of release-ready vesicles during trains of stimuli has long been discussed as a cause of synaptic depression (Liley and North, 1953; Elmquist and Quastel, 1965; Betz, 1970; Kusano and Landau; 1975; see also reviews by Zucker, 1996 and Neher, 1998a). Interestingly, analyses of the kinetic and steady-state behavior of synaptic depression at various stimulation frequencies have provided evidence that the recovery process seems to be enhanced during repetitive activity (Kusano and Landau, 1975; Gingrich and Byrne, 1985).

In the simplest case, this enhancement would come about from the fact that during depression more empty release sites are available for accepting vesicles. A model assuming vesicles to become available for release at a fixed rate per empty release site, however, cannot explain some of the features of synaptic depression observed in various preparations. In a recent study, Worden et al. (1997) have presented the analysis of a model in which each stimulus causes some extra recruitment of new vesicles, in addition to a background of vesicle dynamics at fixed rate constants. With this approach, they were able to simulate many features of facilitation at the lobster neuromuscular junction. They did not specify, however, by what mechanism the extra recruitment is controlled. For some central nervous system synapses, it has recently been reported that presynaptic $[Ca^{++}]_i$ speeds up the recovery from synaptic depression (Stevens and Wesseling, 1998; Wang and Kaczmarek, 1998; Dittman and Regehr, 1998). Such an enhanced recovery after a (partial) depletion of a pool of readily releasable vesicles could be an important regulator of synaptic transmission in depressing synapses, where it could help to counteract the effect of vesicle pool depletion and ensure a certain level of steady-state output during repetitive stimulation.

We explore here the possibility that an enhanced rate of recovery is a consequence of Ca^{++} inflow during an action potential. Approximating the terminal as a "single compartment" with respect to Ca^{++} dynamics (Helmchen et al., 1997; Neher and Augustine, 1992) and assuming that the rate of recruitment of vesicles to empty release sites is proportional to the spatially averaged cytosolic Ca^{++} concentration $[Ca^{++}]_i$ in the terminal, we can simulate some of the features described in the literature and some aspects of our own data on depression at the calyx of Held (v. Gersdorff et al., 1997). However, experiments on the calyx of Held designed to further explore predictions of the model regarding some manipulations of intraterminal $[Ca^{++}]_i$ failed to reproduce these predictions. Also, consideration of the properties of such a single-compartment model leads to the more general conclusion that adding buffers to the terminals, aimed at suppressing Ca^{++} action on vesicle recruitment (which is the accepted means of experimentally addressing such problems), should actually not lead to such suppression at steady state in models in which $[Ca^{++}]_i$ acts linearly on its effectors (see also Neher, 1998b). Rather, for buffers to exert the expected effects, nonlinear Ca^{++} action has to be assumed, or else the action of high $[Ca^{++}]_i$ in spatially restricted domains.

Received for publication 15 April 1999 and in final form 12 July 1999.

Address reprint requests to Dr. Erwin Neher, Abt. Membranbiophysik, Max-Planck-Institut für biophysikalische Chemie, Am Fassberg 11, D-37077 Göttingen, Germany. Tel. +49-551-201-1630; Fax: +49-551-201-1688; E-Mail: eneher@gwdg.de.

0006-3495/99/11/2418/12 $2.00

MATERIALS AND METHODS

Analysis and numerical calculations

The differential equations for the two different models were solved numerically using the integration method of Runge–Kutta. The integrating routines were written and performed with the program IgorPro (Wavemetrics, Lake Oswego, OR). The single compartment model described by Neher and Augustine (1992) and Helmchen et al. (1997) was used to predict the influence of Ca^{++} buffers on the amplitude and the time course of the $[Ca^{++}]_i$ transient, assuming a constant pump rate. Simulations were done on a Macintosh computer.

For the comparison of the theory with the experimental data, a least squares fit was used to minimize the deviation between the prediction and the experimental data. This program was written with MATLAB (Mathworks Inc., Natick, MA).

Slice preparation, electrophysiological recording and $[Ca^{++}]_i$-imaging

Experimental procedures for patch-clamp recordings of the pre- and postsynaptic elements of the calyx of Held synapse in rat brainstem slices closely followed previously described methods (Forsythe, 1994; Borst et al., 1995; v. Gersdorff et al., 1997). Briefly, 200-μm-thick, transverse brainstem slices were made with a vibratome (Campden, Loughborough, England) from 8–11-days-old Wistar rats that were killed by decapitation. Slices were kept at 36°C in a solution composed of (in mM) 125 NaCl, 25 $NaHCO_3$, 1.25 NaH_2PO_4, 2.5 KCl, 2 $CaCl_2$, 1 $MgCl_2$, 25 glucose, 3 myoinositol, 2 Na-pyruvate, 0.4 ascorbic acid (pH 7.4 when bubbled with 95% O_2 5% CO_2). Slices were transferred after a minimum of 30 min to the experimental chamber in an upright microscope (Axioskop, Zeiss, Oberkochen, Germany). Whole-cell patch-clamp recordings were made at room temperature (22–25°C) with a pipette solution containing (in mM) 130 K-gluconate, 20 KCl, 10 Hepes, 4 Mg-ATP, 0.3 Na-GTP, 5 Na_2-phosphocreatine (pH 7.2), using an EPC-9 patch-clamp amplifier (HEKA-Elektronik, Lambrecht, Germany). Afferent fiber stimulation was delivered with a bipolar stimulation electrode. Principal cells of the medial nucleus of the trapezoid body were visualized with a slow-scan CCD imaging camera (see below), using gradient contrast infrared illumination (Luigs and Neumann, Ratigen, Germany).

A brief, presynaptic recording episode of ≈2 minutes was established to preload the calyx with approximately 80–100 μM fura-2. This was done by adding 200 μM fura-2 to the internal solution. Considering the loading time course of the calyces with fura-2 under similar experimental conditions to ours (Helmchen et al., 1997), it is seen that roughly 50% loading is achieved after about 2 min. An alternative estimate of the intraterminal fura-2 concentration can be obtained by analyzing the decay time constant of $[Ca^{++}]_i$(τ_x) after brief Ca^{++} influx, since a strong correlation between τ_x and intracellular fura-2 concentration is expected (Neher and Augustine, 1992; Helmchen et al., 1997). The average value for τ_x from $n = 6$ calyces loaded completely (>5 min) with 80 μM fura-2 was 0.96 ± 0.35 s. This value is in good agreement with the one reported by Helmchen et al. (1997), and can serve as a reference point for a rough estimate of the fura-2 concentration achieved after 2 min preloading (see Table 2). After the preloading episode, the presynaptic patch pipette was withdrawn and a postsynaptic recording was established with internal solution complemented with 5 mM EGTA. Effective series resistance of postsynaptic recordings was 3–4 MΩ after partial compensation with the EPC-9 amplifier. The amplitudes of postsynaptic EPSCs reported here were corrected for the estimated voltage-clamp error as described in Schneggenburger et al. (1999).

$[Ca^{++}]_i$ imaging was performed using a polychromatic light source (TILL photonics, Martinsried, Germany) to excite fura-2 at 357 nm and at 380 nm. The excitation light was attenuated to 10% with a neutral density filter. Fluorescence signals were imaged with a slow-scan CCD camera (TILL photonics) using on-chip binning (8 × 8 pixels) to increase signal-to-noise ratio and temporal resolution (20-ms exposure times with repetition rates of 20 Hz). Spatially averaged $[Ca^{++}]_i$ values were calculated from background-corrected fluorescence values using the equation given by Grynkiewicz et al. (1985). The calibration constants were determined in vitro using thin quartz-glass capillaries, and were confirmed in cellular measurements using bovine chromaffin cells.

RESULTS

The Model

The basic assumption of the model (Fig. 1) is that the final stages of release at a synapse can be approximated by a two-step process,

$$A \underset{k_{-1}}{\overset{k_1([Ca^{++}]_i)}{\rightleftharpoons}} B \xrightarrow{P} C$$

SCHEME 1

Here, the transition A → B can be considered either to be the binding of a vesicle to an empty release site or else the maturation of an already docked vesicle to become release ready. This transition is described by a Ca^{++}-dependent rate constant k_1 ($[Ca^{++}]_i$). We allow this step to be reversible and characterize the backward reaction by a fixed rate constant k_{-1}. Release-ready vesicles can undergo exocytosis (B → C) during an action potential with probability p, such that the synaptic response Y is given by

$$Y = q \cdot n_{B-} \cdot p, \tag{1}$$

where q represents the quantal size and n_{B-} is the number of vesicles (or release sites) in state B immediately before the action potential, n_{B+}, the number of vesicles immediately after the action potential is then given by

$$n_{B+} = (1 - p) \cdot n_{B-}. \tag{2}$$

The time course of n_B in between two action potentials is described by the kinetic equation (according to Scheme 1)

$$\frac{d}{dt} n_B = k_1([Ca^{++}]_i) \cdot n_A - k_{-1} \cdot n_B. \tag{3}$$

We assume here that release in the time interval between two action potentials is negligible. A more general treatment allowing Ca^{++}-dependent release in between two stimuli has been given by Weis (1998).

We discuss two interpretations of such a model. In the first one, states A and B represent different states of maturation of vesicles. We will call this interpretation a vesicle-state model. We consider the simplest form of such a model, in which the number of reserve vesicles n_A is very large, such that it can be considered as constant. Then, the product $k_1 \cdot n_A$ in Eq. 3 can be replaced by an apparent zero-order rate constant k_1^* ($[Ca^{++}]_i$), and the steady-state number $n_{B,b}$ of release-ready vesicles at basal $[Ca^{++}]_i$, $[Ca^{++}]_b$, will be given by

$$n_{B,b} = \frac{k_1^*([Ca^{++}]_b)}{k_{-1}} \equiv \frac{k_{1,b}^*}{k_{-1}}. \tag{4}$$

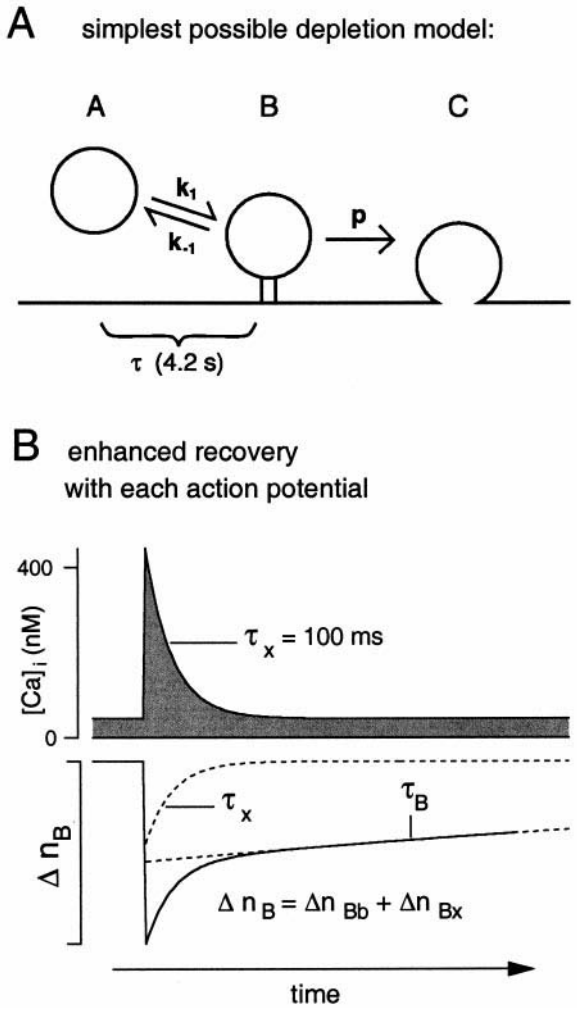

FIGURE 1 The basic features of the model. (*A*) Vesicles are assumed to be released from a release-ready pool B with release probability p during an action potential, and are resupplied from pool A. In the simplest possible depletion model, the refilling rate constant k_1 has a fixed value. (*B*) Enhanced recruitment of vesicles after each action potential. *Upper panel,* decay time course of $[Ca^{++}]_i$ after a single action potential. In the calyx of Held, the $[Ca^{++}]_i$ time constant τ_x is roughly 100 ms in the absence of exogenous Ca^{++} buffers (Helmchen et al., 1997). With the assumption of linear dependence of rate constant k_1 with $[Ca^{++}]_i$, recovery of pool B will proceed with two distinct time constants, τ_x and τ_B (*lower panel;* see Eqs. 24–26).

This interpretation of the model is very similar to the model of Heinemann et al. (1993), which was used to describe secretion of hormones in neuroendocrine cells (see also Smith et al., 1998). For synaptic transmission, it may be more appropriate to interpret state A and B as states of release sites, which can either be in a release-ready state (B), or in a state (A) from which no immediate release can occur (including the possibility that no vesicle is docked). We will refer to this interpretation as the release site model. In this case, it is likely that the total number of release sites n_T is finite and we make the assumption

$$n_A + n_B = n_T . \tag{5}$$

If n_T is constant, we obtain from Eqs. 3 and 5

$$\frac{d}{dt} n_B = k_1([Ca^{++}]_i) \cdot n_T - \{k_1([Ca^{++}]_i) + k_{-1})\} \cdot n_B . \tag{6}$$

The steady-state number $n_{B,b}$ of release-ready sites at basal $[Ca^{++}]_i$ is then given by

$$n_{B,b} = n_T \cdot \frac{k_{1,b}}{k_{1,b} + k_{-1}} . \tag{7}$$

Here, we have implied that there is an unlimited supply of vesicles and that release sites return instantaneously into state A after releasing a vesicle. This interpretation of the model is very similar to the model of Dittman and Regehr (1998), except that we allow vesicle docking to be reversible. The main differences between the models discussed here concern the steady-state value of n_B: in the Dittman and Regehr (1998) model, n_B will always go to its maximum value (all release sites occupied) during long enough resting periods; our release-site model will reach an intermediate steady-state occupancy in between 0 and n_T, as given by Eq. 7, and the vesicle-state model is not limited in the number of release-ready vesicles at rest (due to the simplifying assumption of an infinite reserve pool). The two types of models behave very different with respect to their predictions regarding fluctuations of synaptic responses (Vere-Jones, 1966).

Under conditions of strong depression, the vesicle-state model and the release-site model are formally equivalent, considering Eqs. 6 and 3, since, for $n_B \ll n_T$,

$$k_1([Ca^{++}]_i) \cdot (n_T - n_B) \approx k_1^*([Ca^{++}]_i),$$

with (8)

$$k_1^*([Ca^{++}]_i) = n_T \cdot k_1([Ca^{++}]_i).$$

In the following, we will mostly write the equations for the more complicated release-site model and indicate the simplifications, in analogy to Eq. 8, for the transition to the vesicle-state model.

To further discuss the Ca^{++}- and time-dependence of k_1, we will use the shorter notation $x(t) = [Ca^{++}]_i$. We assume that k_1 is linearly related to $x(t)$ with

$$k_1(t) = k_{1b} \cdot \frac{x(t)}{x_b}, \tag{9}$$

where x_b is the basal $[Ca^{++}]_i$ under resting conditions. This is a further simplification with respect to Heinemann et al. (1993) and Dittman and Regehr (1998), who used a Michaelis–Menten type relationship. However, the different approaches agree for the case that $x(t)$ is smaller than the dissociation constant of the Michaelis–Menten type regulator. The linear approximation, used here, overestimates the pool recovery process with respect to the full Michaelis–Menten case.

The time course of calcium concentration

Several studies (Regehr et al., 1994; Helmchen et al., 1997) have shown that the mean spatial intracellular calcium transient after a single action potential can be written as

$$x(t) = x_o \cdot e^{-t/\tau_x} + x_b \quad \text{for} \quad t > 0, \tag{10}$$

with x_o, the increment of the calcium concentration transient during an action potential, x_b, the basal $[Ca^{++}]_i$, and τ_x, the time constant of the decay of the $[Ca^{++}]_i$ transient.

According to the single compartment model for Ca^{++} buffering (Neher and Augustine, 1992), τ_x and x_o can be expressed as

$$\tau_x = \frac{1 + \kappa_S + \kappa_B}{\gamma} \tag{11}$$

and

$$x_o = [Ca^{++}]_{tot} \cdot \frac{1}{1 + \kappa_B + \kappa_S}, \tag{12}$$

with κ_S, the Ca^{++}-binding ratio of the endogenous Ca^{++} buffer; γ, the pump rate of a Ca^{++} extrusion mechanism, and $[Ca^{++}]_{tot}$, the total Ca^{++} concentration change. κ_B is the Ca^{++}-binding ratio of an experimentally added buffer, such as a Ca^{++} indicator dye. Appendix A gives the corresponding equations for the $[Ca^{++}]_i$ time course during trains of action potentials.

In our analysis, we assume that the mean spatial calcium concentration is too small to elicit release in between stimuli. Rather, we assume that transmitter release is elicited by a delta-function like spike in local calcium concentration close to the membrane during action potentials, resulting in a certain release probability p (see above). Spatial gradients of calcium relax quickly by diffusion and other balancing actions and result in a mean spatial concentration x(t), which we use for calculation of the changes in n_B during interpulse intervals according to Eqs. 3, 9, A1, and A2.

Time course of n_B after a single stimulus

At times long after a stimulus, when $x(t)$ has returned to basal values, Eq. 6 assumes the form

$$\frac{d}{dt} n_B = k_{1b} \cdot n_T - (k_{1b} + k_{-1}) \cdot n_B, \tag{13}$$

with the steady-state solution $n_{B,b}$ according to Eq. 7 and a relaxation toward $n_{B,b}$ according to

$$n_B = n_{B,b} + \text{const} \cdot e^{-t/\tau_B} \quad \text{for} \quad t \gg \tau_x. \tag{14}$$

The recovery time constant τ_B (at basal $[Ca^{++}]_i$) is given by

$$\tau_B = 1/(k_{1b} + k_{-1}). \tag{15}$$

This equation holds for the release-site model. For the vesicle-state model the equivalent equation is:

$$\tau_B = 1/k_{-1}. \tag{16}$$

At earlier times, while $x(t)$ is changing, Eq. 6, using Eq. 7, 9, and Eq. 15 can be written in the form

Release-site model

$$\frac{dy}{dt} = \frac{1}{\tau_B}\frac{x(t)}{x_b} - \left[k_{-1} + k_{1b}\frac{x(t)}{x_b}\right] \cdot y, \tag{17}$$

with $y(t)$ denoting the normalized number of release-ready sites, according to

$$y = n_B/n_{B,b}. \tag{18}$$

This is an inhomogeneous differential equation of first-order, linear in y and dy/dt.

We can rewrite Eq. 17 as

$$\frac{dy}{dt} + G(t) \cdot y = H(t) \tag{19}$$

with

$$G(t) = k_{-1} + k_{1b} \cdot \frac{x(t)}{x_b}, \tag{20}$$

$$H(t) = \frac{1}{\tau_B}\frac{x(t)}{x_b}. \tag{21}$$

The general solution of Eq. 19 in any time interval $t_1 < t < t_2$ that does not contain a stimulation, is given by

$$y(t) = \left\{ y(t_1) + \int_{t_1}^{t} H(\tau) \cdot \exp\left[\int_{t_1}^{\tau} G(u)\, du\right] d\tau \right\} \cdot \exp\left[-\int_{t_1}^{t} G(\tau)\, d\tau\right] \tag{22}$$

(Bronstein and Semendjajew, 1991).

Evaluating the integrals in Eq. 22 is quite involved due to the occurrence of a term proportional to $x(t)$ in $G(t)$. This term is missing in the formulation of the vesicle-state model, which leads to much simpler expressions. Consideration of Eqs. 17 and 20, however, allows the conclusion that the problematic second term in $G(t)$ should not be of much relevance in most situations of interest. For instance, for times long after a stimulus, when $x(t) \approx x_b$, we can set $G(t) \approx k_{-1} + k_{1b} = 1/\tau_B$. For times short after a stimulus, when the synapse is depressed ($y \ll 1$) the product $G(t) \cdot y$ is small with respect to the first term in Eq. 17. Therefore, the time dependence of $x(t)$ is of relevance only for situations in which τ_x is so long that substantial recovery of n_B can occur while $[Ca^{++}]_i$ is still larger than the resting $[Ca^{++}]_i$. In that case, the neglect of the time dependence of $G(t)$ will lead to an overshoot of n_B above n_T. Thus, for $y \ll 1$, we can evaluate n_B according to a simplified equation, which is identical to the equivalent equation of the vesicle-

state model and its corresponding definition of τ_B (Eq. 16):

$$\frac{dy}{dt} = \frac{1}{\tau_B}\left(\frac{x(t)}{x_b} - y\right). \quad (23)$$

Further justification of this simplification will be given below, where the time course of n_B obtained by solving Eq. 23 will be compared with a numerically calculated one according to Eq. 17 (see Fig. 3, *B* and *C*). Solving Eq. 23 for a single stimulus and the initial condition $n_B(0) = n_{B,b} \cdot (1 - p)$, we obtain

$$n_B(t) = n_{B,b} - \Delta n_{Bb} \cdot e^{-t/\tau_B} - \Delta n_{Bx} \cdot e^{-t/\tau_x}, \quad (24)$$

with

$$\Delta n_{Bb} = n_{B,b} \cdot \left(p - \frac{x_o}{x_b} \cdot \frac{\tau_x}{\tau_B - \tau_x}\right) \quad (25)$$

and

$$\Delta n_{Bx} = n_{B,b} \cdot \frac{x_o}{x_b} \cdot \frac{\tau_x}{\tau_B - \tau_x}. \quad (26)$$

This solution reveals that the time dependence of n_B is a superposition of two different exponential recovery processes: one with the exponential time constant τ_B and one with τ_x. This behavior is illustrated in Fig. 1 *B*. The contribution with the label *x* is due to the calcium transient and the extra recruitment of vesicles at elevated calcium concentration. Solutions of relative pool size, $n_B(t)/n_{B,b}$ and $x(t)$ for trains of stimuli are given in Appendix A.

Comparison between model predictions and experimentally observed depression at the calyx of Held

v. Gersdorff et al. (1997) studied synaptic depression at the calyx of Held for pulse trains in the range of 0.2 to 10 Hz. They found that recovery from depression, in a time window of 0.5–16 s, in which $[Ca^{++}]_i$ is likely to have returned to basal values, proceeds with an exponential time course with time constant $\tau_B = 4.2$ s. The relative steady-state excitatory postsynaptic current (EPSC)-amplitude during depression was found to be correlated with the amplitude of the first EPSC (see Fig. 2 *B* of v. Gersdorff et al., 1997). To analyze the kinetics of depression, we subdivided the data set for 10 Hz stimulation into a group of synapses with small EPSC amplitudes (4.02 ± 1.17 nA, $n = 5$ cells, Fig. 2 *A*1) and another group with large EPSC amplitudes (12.53 ± 1.6 nA, $n = 4$ cells, Fig. 2 *A*2). Although the subdivision in two groups is somewhat arbitrary, it allows taking into account a possible variability of depression parameters between cells.

The theory, as outlined above, very accurately describes both the time course into depression during individual trains, and the steady-state depression as a function of frequency. The fits in Fig. 2, *A* and *B* use Eqs. A6 and A8, respectively, as the theoretical prediction for the data points. In these fits, with τ_B given by the separate experiments of v. Gersdorff et al. (1997), the only free parameters were p, x_o/x_b, and τ_x. For the latter two parameters, which reflect relative amplitude and time constant of the $[Ca^{++}]_i$-transient, the fit resulted in values compatible with measurements of $[Ca^{++}]_i$. For instance, the fits of Fig. 2, *A*1 and *A*2 gave τ_x values of 136 and 75 ms, respectively, which compare favorably with the range of 78 ms $< \tau_x <$ 112 ms given by Helmchen et al. (1997). The value of p, estimated both from the fits of the simple depletion model with fixed time constant of recovery (see legend of Fig. 2 for details) and from fits of the vesicle-state model, were found to be 0.3 for the group of cells with small EPSC, and 0.6 for the group of large EPSC amplitudes. The difference in p between the two cell groups reflects the observed difference in the time course and steady-state value of depression (see Fig. 2, *A*1 and *A*2). Furthermore, fits using the parameter $x_o/x_b \cdot \tau_x/(\tau_B - \tau_x)$ as freely variable (see Table 1) indicate that ≈10% of the total pool of vesicles is recovered during the period of enhanced recovery, because $x_o \cdot \tau_x \approx 0.1 \cdot x_b \cdot (\tau_B - \tau_x)$.

In contrast, a theory with fixed rate constant (vesicle recovery independent of $[Ca^{++}]_i$) could not fit these data. Fits that were appropriate for short times or low frequencies in Fig. 2, *A* and *B*, respectively, did not reproduce the relatively high plateau at long times or higher frequencies (*dashed lines* in Fig. 2, *A* and *B*). In fact, many simple models would predict a steady-state depression level inversely proportional to frequency (see legend of Fig. 2; Worden et al., 1997; Tsodyks and Markram, 1997). The deviation from this expectation above 2 Hz is clearly shown in Fig. 2 *B*.

We were interested in designing experiments to test the model predictions for the case of added Ca^{++} buffers. Fig. 3 *A* shows the model predictions for the build-up of $[Ca^{++}]_i$ during a train of stimuli (see Appendix A for the relevant equations). In the presence of extra buffer (80 μM fura-2), this buildup is slower, and excursions of $[Ca^{++}]_i$ in between stimuli are smaller. However, once the steady state is reached, temporal averages of $[Ca^{++}]_i$ are quite similar to those of the control case. Following the train, $[Ca^{++}]_i$ decays rapidly in the absence of buffers, but slower in the presence of 80 μM fura-2 (Fig. 3 *A*). This prediction is born out in the $[Ca^{++}]_i$ measurement of Fig. 4 *A* (see below).

Figure 3 *B* displays the numerically integrated exact solutions for the release-site model according to Eq. 17 (see figure legend and below for choice of parameters), and Fig. 3 *C* shows the analytical solutions according to Eq. A5 (which are the correct ones for the vesicle-state model). The model predicts that the path into depression should be faster with added buffer, and should go through a minimum before reaching steady state (see Fig. 3, *B* and *C*), because there is initially less extra recovery due to the smaller $[Ca^{++}]_i$-increment. As $[Ca^{++}]_i$ builds up during a train, however, the same steady-state level of depression is reached, because in steady state, the time-averaged $[Ca^{++}]_i$ is identical under control and buffer situations. The difference between the

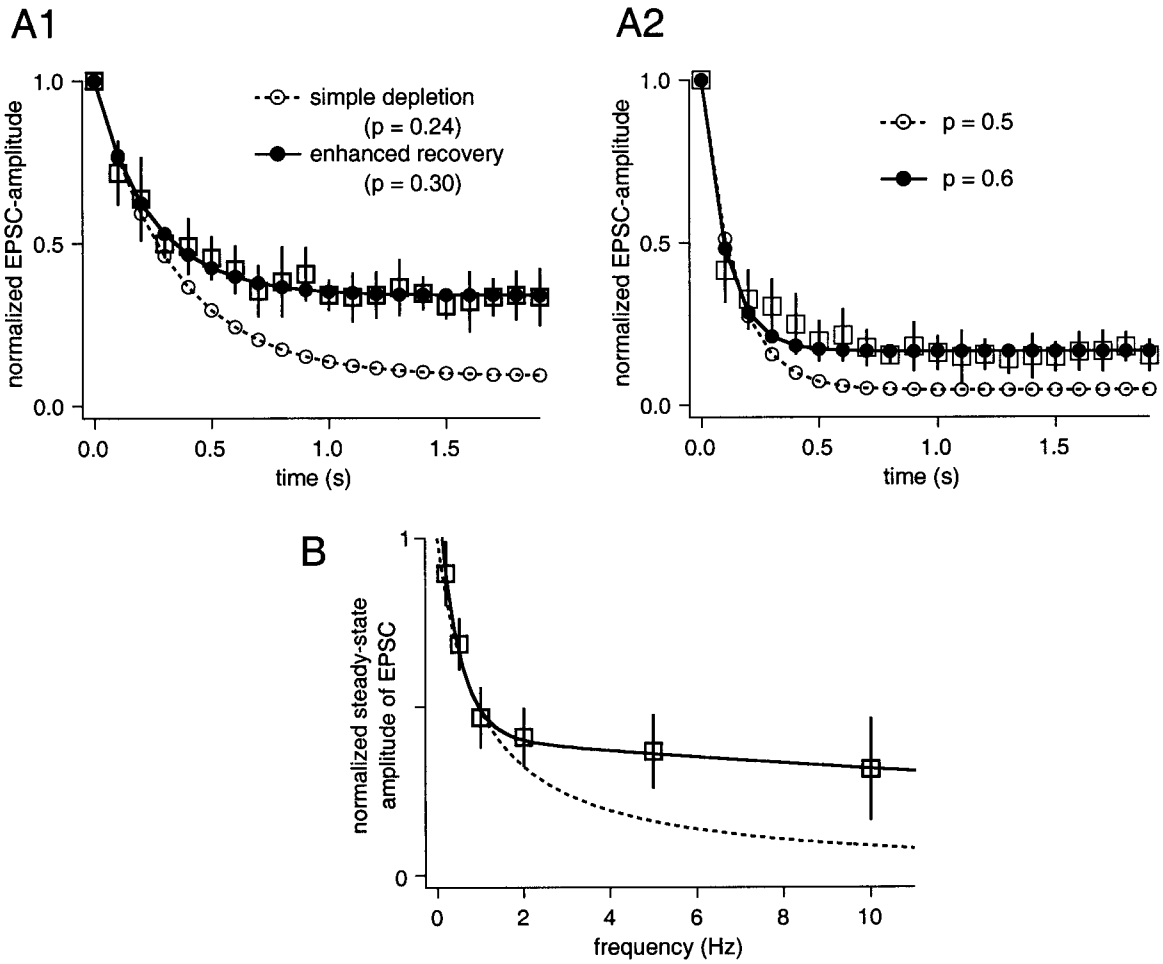

FIGURE 2 A model that assumes a period of enhanced recovery after each action potential provides an adequate fit of depression at the calyx of Held synapse. (*A*) Average values of normalized EPSC-amplitudes during 10 Hz trains, measured in MNTB principal neurons (*open squares*). The data was subdivided in two groups according to the amplitudes of the first EPSCs, which had average values of 4.0 ± 1.2 nA for *A*1 (n = 5 cells) and 12.5 ± 1.6 nA for *A*2 (n = 4 cells). The fits of the vesicle-state model are superimposed (*filled symbols;* Eq. A6). The predictions of the simplest possible depletion model *(open symbols),* with a fixed recovery time constant τ_B were calculated recursively according to:

$$n_{B[i+1]} = (1 - p)n_{B[i]} + \{n_{B[1]} - (1 - p)n_{B[i]}\}\{1 - e^{-\Delta t/\tau B}\},$$

where i was incremented from 1, 2, . . . , 20 stimuli, $n_{B[1]}$ was set to 1 to yield normalized pool size, and τ_B was 4.2 s. This calculation simply assumes that the recovered fraction in between stimuli is proportional to the deviation of pool size from its steady-state value. Release probability p was varied to fit the first three data points. Note that the vesicle-state model, which assumes a short period of faster recovery (see Fig. 1 *B*) gives slightly larger values for p, as expected. (*B*) Steady-state EPSC-amplitudes as a function of frequency. Here, small and large EPSC amplitudes were pooled, and this data set is the same as the one in Fig. 2 *A* of v. Gersdorff et al. (1997). The solid line represents a fit of the vesicle-state model according to Eq. A8. The dotted line is drawn according to the steady-state expression for the simplest possible depletion model, $y = 1/(1 + fp\tau_B)$, with f, stimulation frequency, τ_B = 4.2 s and p = 0.25 for this data set. Note that this relation, with a fixed rate constant for pool refilling, does not explain the plateau in steady-state synaptic output observed at frequencies >2 Hz.

two predicted time courses is not very pronounced, however. In contrast, following a stimulus train, the model predicts recovery from depression to be much more rapid under buffer condition as compared to control (*arrows* in Fig. 3, *B* and *C*). In the case of the vesicle-state model, there should be even a rebound overshoot in the size of the readily-releasable pool (see Fig. 3 *C*). The faster time course of recovery from depression is due to the slow decay of $[Ca^{++}]_i$ in the presence of buffer.

To experimentally test the model predictions, an estimated concentration of 80–100 μM fura-2 (see Materials and Methods) was loaded via a patch-pipette into presynaptic calyces (Fig. 4). At this concentration, fura-2 should not reduce the release probability of the synapse [see Borst et al. (1995) for the case of 50 μM BAPTA]. However, due to the weak endogenous Ca^{++}-buffering capacity of calyces ($\kappa_S \approx 40$; Helmchen et al., 1997), fura-2 is expected to have a large influence on the amplitude (x_o) and time course (τ_x) of spatially averaged $[Ca^{++}]_i$ signals. After the preloading of the calyx and removal of the first pipette, a recording of the postsynaptic cell was established with a second pipette. The kinetics of depression of EPSCs were measured with

TABLE 1 Estimation of the relative amount of extra recovery from fits with the quantity $x_o/x_b \cdot \tau_x/(\tau_B - \tau_x)$ as a fit parameter

Frequency (Hz)	$x_o/x_b \cdot \tau_x/(\tau_B - \tau_x)$	Number of Cells
10	0.10 ± 0.03	10
5	0.10 ± 0.02	8
2	0.13 ± 0.05	5

trains of $n = 20$ stimuli at 10 Hz, followed by single test stimuli at times between $0.5 < \Delta t < 8$ s after the train, to monitor the recovery from depression. Simultaneously, presynaptic $[Ca^{++}]_i$ responses were measured using the fura-2 fluorescence signals (see Fig. 4 *A*).

Despite the severalfold prolonged decay of $[Ca^{++}]_i$ with respect to the control situation (*thin line* in Fig. 4 *A*; Helmchen et al., 1997), the fraction of recovery that occurred at Δt of 2 s (Fig. 4 *B*) was unchanged with respect to the control conditions in the absence of added Ca^{++} buffer (v. Gersdorff et al., 1997). The complete time course of recovery from depression, measured with $n = 17$ pairs of conditioning trains and test stimuli, could be well fitted by a single exponential with time constant, $\tau = 3.8$ s (Fig. 4 *D*). Similar results were obtained in three cells (see Table 2). Additionally, Fig. 4 *C* shows that the kinetics into depression were unchanged, i.e., no minimum of EPSC amplitudes was observed before reaching steady state, contrary to the predictions shown in Fig. 3, *B* and *C*. Thus, the kinetic changes predicted by the models, which include a Ca^{++}-dependent increase of vesicle pool recovery (see Fig. 3, *B* and *C*) were not observed experimentally. At present, however, we cannot exclude that presynaptic fura-2 induced small changes in the amplitudes of the first EPSC or of EPSCs during the steady-state phase of depression, since there are no preinjection control values for the type of experiment shown in Fig. 4.

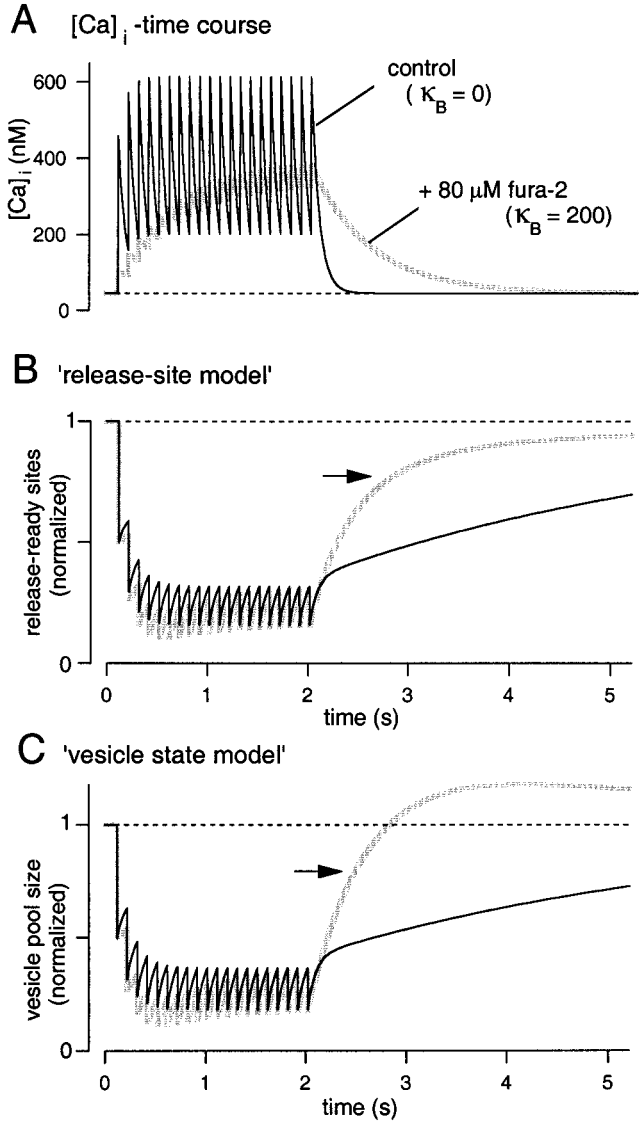

FIGURE 3 Simulations of $[Ca^{++}]_i$ and vesicle pool size during 10 Hz action potential trains. (*A*) $[Ca^{++}]_i$ was calculated according to the single-compartment model (Eqs. 11, 12, A2). The values of κ_s and γ were 30 and 400 s^{-1}, respectively, close to the values reported by Helmchen et al. (1997). For the simulation of added Ca^{++} buffer, a constant value of $\kappa_B = 200$ was used. (*B*) Time-course of the relative number of release-ready sites, according to the release-site model, with $k_{1b} = 0.15\ s^{-1}$ in Eq. 17. (*C*) Time-course of the relative number of ready-releasable vesicles, according to the vesicle-state model (Eq. 23). In both *B* and *C*, the release probability *p* was set to 0.5. Note that, in both models, the addition of small concentrations of exogenous buffer (*thick grey lines*) leads to a significant enhancement of the rate of recovery from depression (see *arrows*) with respect to the control condition *(thin lines).* In addition, a transient overfilling of the vesicle pool size occurs in the case of the vesicle-state model, because here the number of release sites is not limited (see Results).

DISCUSSION

In this study, we have explored the predictions of a theoretical model designed to describe kinetic complexities of synaptic depression at various types of synapses (Elmquist and Quastel, 1965; Stevens and Wesseling, 1998). The basic assumption of the model is that fast synaptic depression is caused by depletion of a readily-releasable pool of synaptic vesicles, compatible with the results from several recent experimental studies on the calyx of Held (v. Gersdorff et al., 1997; Wang and Kaczmarek, 1998; Borst and Sakmann, 1999; Schneggenburger et al., 1999; Wu and Borst, 1999). We show that the simplest possible depletion model, incorporating only two parameters (a fixed recovery time constant τ and a constant value of release probability *p*), does not give a good fit of depression, because it leads to an underestimation of steady-state synaptic output for stimulation frequencies above 2 Hz (see Fig. 2). This led us to postulate that, during trains of synaptic activity, an extra recovery of synaptic vesicles must take place after each action potential, as has been done previously for other preparations (Kusano and Landau, 1975; Elmquist and Quastel, 1965; Worden et al., 1997; see also Dittman and Regehr, 1998 and discussion therein). Indeed, with an extra recovery with time constant of 100 ms and capacity of ≈10% of the nondepressed synaptic response (see Table 1),

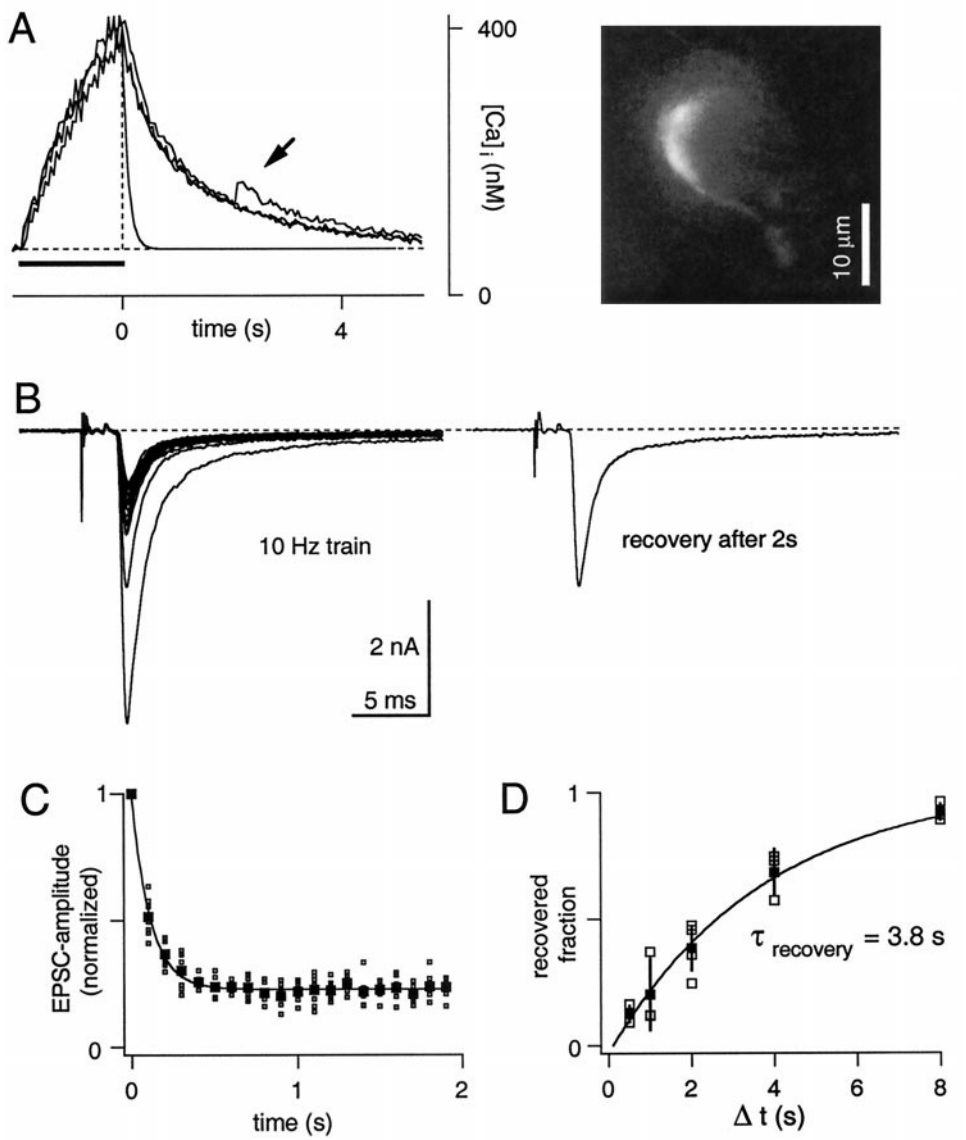

FIGURE 4 Synaptic depression in the presence of 80–100 μM presynaptic fura-2 does not show kinetic changes. (*A*) Presynaptic $[Ca^{++}]_i$-transients in response to 10 Hz trains. In one case *(arrow),* a single stimulus was delivered 2 s after the end of the conditioning train. The inset shows a fura-2 fluorescence image of the calyx used in this experiment. (*B*) Example of postsynaptic EPSCs in response to a 10 Hz train *(left panel)* and in response to a single stimulus 2 s later *(right panel).* Note that these EPSCs correspond to the presynaptic $[Ca^{++}]_i$-trace labeled by the arrow in *A*. (*C*) Way into depression. EPSC amplitudes were normalized to the first amplitude, and the average of $n = 7$ trains *(filled symbols)* was fitted with an exponential. (*D*) Time course of recovery from depression. The average data points *(filled symbols)* were fitted with an exponential function with $\tau = 3.8$ s. Cell Ja09A.

the kinetic and steady-state properties of depression were well described for various stimulation frequencies (see Fig. 2). In our model this extra recovery was assumed to be due to accelerated recruitment of vesicles to a release-ready pool while $[Ca^{++}]_i$ is elevated during short periods following an action potential (see also Dittman and Regehr, 1998). Specifically, we assumed that the $[Ca^{++}]_i$ transient, as measured by Ca^{++} indicator dyes, can be used as a parameter to describe the acceleration of recruitment. This assumption implies linear $[Ca^{++}]_i$ dynamics of the terminal within a certain range of $[Ca^{++}]_i$ changes, as demonstrated experimentally by Helmchen et al. (1997) in the calyx of Held. For such linear models, it can be generally shown that addition of Ca^{++} buffers does not influence Ca^{++}-dependent processes at steady state, but only changes the time course toward steady state (Neher, 1998b). However, our experiments at the calyx of Held, designed to change such transient properties by adding Ca^{++} buffers, did not lead to changes in recovery from depression, as predicted by the model, in spite of profound changes in the Ca^{++} signal. Thus, we are not in a position to identify the mechanism(s) causing the complexities in the kinetics of depression. Nevertheless, we think it is of interest to explore the implications of our findings for models of Ca^{++}-dependent synaptic short-term plasticity and to discuss the consequences of

TABLE 2 Summary of experiments in which presynaptic calyces were preloaded with an estimated concentration of 80–100 μM fura-2

Cell code	τ^*_{Ca} ($= \tau_x$) (s)	$\tau_{recovery}$[#] ($= \tau_B$) (s)	EPSC amplitude[§] (nA)
De17A	0.85	4.2	-1.92 ± 0.4
Ja07C	0.42	5	-8.03 ± 1.28
Ja09A	1.65	3.8	-4.56 ± 0.4

*Recovery time constant of $[Ca^{++}]_i$ measured after single, presynaptic action potentials.

[#]Recovery time constant from depression, measured as in Fig. 4 *D*.

[§]Average values of first, nondepressed EPSC amplitudes.

the assumption of linearity. Particularly, we ask the question whether the negative result speaks against a Ca^{++}-dependent recruitment of vesicles altogether or else points toward nonlinear (or spatially localized) Ca^{++} effects.

The role of presynaptic $[Ca^{++}]_i$ for the induction of synaptic short-term enhancement, such as facilitation; or augmentation and post-tetanic potentiation on longer time scales, is well established [Katz and Miledi, 1968; Rahamimoff, 1968; Zucker, 1974; Charlton et al., 1982; Swandulla et al., 1991; Kamiya and Zucker, 1994; Delaney and Tank, 1994; Regehr et al., 1994; Atluri and Regehr, 1996; see Fisher et al. (1997) and Zucker (1999) for recent reviews]. However, the role of presynaptic $[Ca^{++}]_i$ in the processes that govern recovery from synaptic depression has not been studied as extensively. At the squid giant synapse, injections of the slow Ca^{++} buffer, EGTA, did not alter the time course of recovery from depression, although it did affect augmentation (Swandulla et al., 1991). For various central nervous system synapses, it has recently been shown that manipulations of Ca^{++} influx (by blockers of voltage-gated Ca^{++} channels) and of presynaptic $[Ca^{++}]_i$ (by the membrane-permeable Ca^{++} chelator, EGTA-AM) affect the recovery rate from synaptic depression, suggesting that increases in $[Ca^{++}]_i$ associated with presynaptic action potentials speed-up the refilling-rate of a readily releasable pool of synaptic vesicles (Wang and Kaczmarek, 1998; Dittman and Regehr, 1998; Stevens and Wesseling, 1998). However, in all these studies, $[Ca^{++}]_i$ was manipulated by indirect means and could not be measured simultaneously. The calyx of Held, in contrast, allows precise control and measurement of $[Ca^{++}]_i$. Unfortunately, however, the Ca^{++} effect seems to be elusive when looked for under such defined conditions. The question remains whether more drastic changes in $[Ca^{++}]_i$ might have revealed an effect (although the model predicted readily identifiable changes).

Buffer effects in linear systems

It is well recognized that injecting Ca^{++} buffer into a cell only transiently changes the basal $[Ca^{++}]_i$ level, because, eventually, the cell will return to its resting level, which is governed by Ca^{++} pumps and fluxes at rest. However, for Ca^{++} transients following a short episode of Ca^{++} influx, a certain type of noneffect of buffer additions has to be postulated as well. It has been shown, both experimentally (Helmchen et al., 1997) and theoretically, using a single-compartment model with a linear Ca^{++}-extrusion rate, that the area under such a $[Ca^{++}]_i$ signal stays constant when adding Ca^{++} buffers to the cytosol (Neher and Augustine, 1992; Helmchen et al., 1997). This is because the time constant of such a transient lengthens by the same factor as the amplitude decreases. More generally, it can be readily shown that the time integral $\int [Ca^{++}]\, dt$ is invariant when buffer is added, no matter whether a fast buffer is used, which just lengthens the time constant of the transient, or else multiple buffers or slow buffers are used, which results in a double or multiexponential time course (Neher, 1998b). In pulse trains, therefore, a steady state in $[Ca^{++}]_i$ is reached that depends on this integral and not on the exact time dependence of the individual responses. Also, it is shown in Appendix B that the extra recruitment of vesicles following a single action potential does not depend on the exact waveform of the Ca^{++}-transient, but rather on its integral, given that the $[Ca^{++}]_i$ transient is short with respect to τ_B, the time constant of pool recovery.

After trains of stimuli, $[Ca^{++}]_i$ will relax back to baseline more slowly in the presence of added Ca^{++} buffer (see Fig. 3 *A*), a prediction that is confirmed by the experimentally measured decay of $[Ca^{++}]_i$ (Fig. 4 *A*). Linking the recovery rate k_1 to the spatially averaged $[Ca^{++}]_i$ level, as done in the models presented here and elsewhere (Dittman and Regehr, 1998), should therefore produce a prolonged phase of accelerated recovery from depression, when a fast Ca^{++} buffer is added to the presynaptic cytosol. This is borne out by the numerical calculations (see Fig. 3, *B* and *C*). Indeed, one of the two types of models formulated here, the vesicle-state model, predicts a rebound overshoot in the size of the readily releasable pool under these conditions (see Fig. 3 *C*).

The calyx of Held

The experimental finding that the recovery time course from depression at the calyx of Held (see Fig. 4 and Table 2) was not affected by the presence of presynaptic Ca^{++} buffer shows that $[Ca^{++}]_i$, in the range of 50–500 nM, does not significantly affect the rate of vesicle refilling at this synapse. However, this result does not rule out a Ca^{++}-dependent step in vesicle refilling altogether. It might indicate that Ca^{++} acts at higher concentrations, possibly by a nonlinear mechanism and in a spatially restricted fashion. Both theoretical (Chad and Eckert, 1984; Simon and Llinás, 1985; Yamada and Zucker, 1992; Roberts, 1994; Naraghi and Neher, 1997) and experimental studies (Heidelberger et al., 1994; Llinás et al., 1995; Schneggenburger et al., 1999) indicate that the Ca^{++} concentration in the immediate vicinity of the release site rises to levels of at least 10 μM or higher, and collapses rapidly when Ca^{++} channels close within less than 1 ms after termination of the action potential (Llinás et al., 1982; Borst and Sakmann, 1996). This fast Ca^{++} spike, besides driving the vesicle fusion, could be responsible for short bouts of extra-recruitment of vesicles to the release-ready pool. This would explain the absence of an effect of 80 μM fura-2 on the kinetics of depression, because it was shown that 50 μM BAPTA, a Ca^{++} chelator with similar kinetic properties as fura-2, did not reduce transmitter release at the calyx of Held (Borst et al., 1995), and therefore probably did not change the local $[Ca^{++}]_i$ signal triggering transmitter release. However, such an explanation would also imply that the extra recruitment of vesicles following an action potential is confined to a time interval similar in length to that of transmitter release. It will therefore be difficult to distinguish experimentally between

a nonlinear or spatially restricted Ca^{++} effect on recruitment, and other consequences of transmitter release. Furthermore, recent data indicate that release probability of newly recruited vesicles is strongly reduced for some period of time following strong stimulation (Wu and Borst, 1999). This finding may provide alternative explanations for the deviations from simple models of recovery from depression at the calyx of Held.

Models of synaptic depression and augmentation

We describe here two variants of a model of Ca^{++}-dependent recruitment of vesicles to a release-ready pool. We emphasize the kinetics of recovery from depression, because this aspect can be readily tested at the calyx of Held. However, Ca^{++}-dependent recruitment of vesicles will also lead to changes in the steady-state size of the pool, if the process of vesicle recruitment is reversible. We assume such reversibility in both variants of our model. Thus, our model will display augmentation/potentiation and a more longlasting form of depression (Zucker, 1999), when basal $[Ca^{++}]_i$ undergoes slow fluctuations in the positive or negative direction, respectively (Eqs. 4 and 7). In this respect, our models differ from that of Dittman and Regehr (1998), in which vesicle recruitment is unidirectional, such that, after long enough periods of rest, all release sites will be occupied. The two variants of our model differ with respect to the degree to which augmentation can take place. Whereas the release-site model sets an upper limit (n_T, see Eq. 7) to the size of the release-ready pool, the vesicle-state model has no such upper bound, as long as the reserve pool of vesicles (assumed to be infinite) is large. The three types of model also present very different behavior with respect to fluctuations of synaptic responses. The model by Dittman and Regehr (1998) will show simple binomical fluctuations, if sufficient time is allowed between successive stimuli for the pool to refill to a constant number of vesicles. The vesicle-state model, in contrast, will show Poisson statistics (Vere-Jones, 1966), whereas the release-site model will show a compound binomical response (Quastel, 1997), unless basal $[Ca^{++}]_i$ is high enough to completely fill the available sites in the pauses between stimuli. Thus, a distinction between some aspects of these models should be possible, irrespective of the question by what mechanism the rate of vesicle recruitment is controlled.

APPENDIX A: EQUATIONS FOR THE CASE OF REPETITIVE STIMULATION

The time course of $[Ca^{++}]_i$ during trains of stimuli

During repetitive stimulation at fixed intervals Δt, assuming that each action potential evokes the same Ca^{++} influx (see Borst and Sakmann, 1999), and assuming additivity of the resulting $[Ca^{++}]_i$-transients, Eq. 10 becomes

$$x(t) = x_o \cdot \sum_{v=1}^{n} \exp\left(-\frac{t-(v-1)\Delta t}{\tau_x}\right) + x_b \qquad \text{(A1)}$$

$$= x_o \cdot \exp(-t/\tau_x) \cdot f_n(\Delta t/\tau_x) + x_b\,, \qquad \text{(A2)}$$

with

$$f_n\left(\frac{\Delta t}{\tau_x}\right) = \frac{\exp(n\Delta t/\tau_x) - 1}{\exp(\Delta t/\tau_x) - 1} \qquad \text{(A3)}$$

valid for $(n-1)\,\Delta t \le t \le n\Delta t$. The time origin in Eqs. A1 and A2 is given by the first stimulus. The accumulation is strongly dependent on the stimulation frequency $1/\Delta t$ and increases with higher frequencies (Regehr et al., 1994; Helmchen et al., 1997).

The time course of n_B during trains of stimuli

The differential Eq. 17 and its simplified form Eq. 23 describe the development of $n_B(t)$ during time intervals without stimulation. To find the time-course for $n_B(t)$ during trains of stimuli with constant frequency $1/\Delta t$, we solve Eq. 17 or Eq. 23 separately in the time intervals $(n-1)\,\Delta t < t < n\Delta t$, using Eqs. A1–A3 for $x(t)$.

If we use the abbreviation

$$F_n(\Delta t/\tau_x) \equiv \frac{x_o}{x_b} \cdot f_n(\Delta t/\tau_x) \cdot \frac{\tau_x}{\tau_B - \tau_x}\,, \qquad \text{(A4)}$$

the solution of Eq. 23 simplifies to

$$y(t) = 1 + \Bigg((1-p)\cdot y_{n-1} - 1 \qquad \text{(A5)}$$

$$- F_n\left(\frac{\Delta t}{\tau_x}\right) \cdot \left(\exp\left(-\frac{(n-1)\Delta t}{\tau_B}\right) - \exp\left(-\frac{(n-1)\Delta t}{\tau_x}\right)\right)$$

$$\cdot \exp\left(-\frac{(t-(n-1)\Delta t)}{\tau_B}\right)\Bigg)$$

$$+ F_n\left(\frac{\Delta t}{\tau_x}\right) \cdot [\exp(-t/\tau_B) - \exp(-t/\tau_x)]$$

$$\text{for} \quad (n-1)\cdot\Delta t \le t \le n\cdot t,$$

where y_{n-1} is the quantity $n_B/n_{B,b}$ immediately before stimulus n. The initial value for n_B at time 0 (immediately following the first stimulus) is $n_{B,b}\cdot(1-p)$, because we assume that n_B was at its basal value before the pulse train and that $n_{B,b}\cdot p$ vesicles were released during the first stimulus, according to Eq. 1. Correspondingly $y(t=0)$ is equal to $1-p$.

We link individual time intervals as described above (Eq. 2), by assuming that each stimulus releases p times the number of release-ready vesicles n_{B-}, which exist immediately preceding the stimulus. The number at the end of the interval, which we call y_n for stimulus $n+1$ can be calculated recursively from y_{n-1}, according to

$$y_n \equiv \frac{n_B(n\Delta t)}{n_{B,b}}$$

$$= 1 - \left(1 - \{1-p\}\cdot y_{n-1} - \frac{1-e^{-n\Delta t/\tau_x}}{1-e^{-\Delta t/\tau_x}} \cdot \frac{\Delta n_{Bx}}{n_{B,b}}\right) \cdot e^{-\Delta t/\tau_B}$$

$$- \frac{1-e^{-n\Delta t/\tau_x}}{1-e^{-\Delta t/\tau_x}} \cdot \frac{\Delta n_{Bx}}{n_{B,b}} \cdot e^{-\Delta t/\tau_x} \quad \text{for} \quad n \ge 1. \qquad \text{(A6)}$$

Synaptic strength Y_{n+1} is then given according to Eq. 1 as

$$Y_{n+1} = q \cdot y_n \cdot n_{B,b} \cdot p. \quad \text{(A7)}$$

If we let the number of stimuli n in a train go to infinity, we get from Eq. A6 and Eq. 18

$$n_{B,\infty} = \frac{n_{B,b} - \left(n_{B,b} - \frac{\Delta n_{Bx}}{1 - e^{-\Delta t/\tau_x}}\right) \cdot e^{-\Delta t/\tau_B} - \frac{\Delta n_{Bx}}{1 - e^{-\Delta t/\tau_x}} \cdot e^{-\Delta t/\tau_x}}{1 - (1 - p) \cdot e^{-\Delta t/\tau_B}}. \quad \text{(A8)}$$

This equation provides a direct relation between the steady-state size of pool B and the release probability p. The value $n_{B,\infty}$ is proportional to the postsynaptic response at steady state and, therefore, represents the steady-state level of depression during a long train of stimuli. Time courses of $x(t) = [Ca^{++}]_i$ according to Eq. A1 are plotted in Fig. 3 *A*, and corresponding time courses of $n_B(t)$ are plotted in Fig. 3 *B* and *C* for a control case and for the case of added Ca^{++} buffer (fura-2).

Examples of the time course of n_B in two limiting cases

Simplified forms of the preceding equations can be obtained for high frequencies ($\Delta t \ll \tau_x$),

$$n_{B,n} = n_{B,n-1} \cdot (1 - p) + (1 - e^{-n\Delta t/\tau_x}) \cdot \Delta n_{Bx} \quad \text{(A9)}$$

and

$$n_{B,\infty} = \Delta n_{Bx}/p. \quad \text{(A10)}$$

For low frequencies ($\Delta t \gg \tau_x$), we obtain

$$n_{B,n} = n_{B,b} - [n_{B,b} - n_{B,n-1} \cdot (1 - p) - \Delta n_{Bx}] \cdot e^{-\Delta t/\tau_B}, \quad \text{(A11)}$$

$$n_{B,\infty} = \frac{n_{B,b} - [n_{B,b} - \Delta n_{Bx}] \cdot e^{-\Delta t/\tau_B}}{1 - (1 - p) \cdot e^{-\Delta t/\tau_B}}. \quad \text{(A12)}$$

APPENDIX B: Ca^{++}-DEPENDENCE OF CUMULATIVE CHANGES IN POOL SIZE

To discuss the dependence of changes in pool size on $[Ca^{++}]_i$, we integrate Eq. 23 over a time interval $[t_1, t_2]$, and see that the net increase in normalized pool size y ($= n_B/n_{B,b}$), during this interval, is given by

$$y(t_2) - y(t_1) = \int_{t_1}^{t_2} \frac{dy}{dt} \cdot dt = \frac{1}{x_b \cdot \tau_B} \left(\int_{t_1}^{t_2} x(t) dt - x_b \int_{t_1}^{t_2} y(t) dt \right). \quad \text{(B1)}$$

We will first consider the steady-state pool size during a train of stimuli. During steady state, it has to be postulated that the same number of vesicles are recruited in the interval between two stimuli as are released during an action potential. Applying Eq. B1 to the interval between two action potentials with length Δt, we obtain

$$p \cdot y_\infty = \frac{1}{x_b \cdot \tau_B} (\Delta t \cdot \overline{x(t)} - x_b \cdot \Delta t \cdot \overline{y(t)}). \quad \text{(B2)}$$

Here y_∞ denotes the value of y shortly before a stimulus, and $\overline{x(t)}$ and $\overline{y(t)}$ are the time averages of x and y at steady state. From this, y_∞ and synaptic strength (which is proportional to y_∞) can be readily calculated,

$$y_\infty = \frac{\Delta t}{x_b} \cdot \frac{\overline{x(t)}}{\tau_B \cdot p + \Delta t \cdot (\overline{y(t)}/y_\infty)} \approx \frac{\Delta t}{x_b} \cdot \frac{\overline{x(t)}}{\tau_B \cdot p + \Delta t}. \quad \text{(B3)}$$

This approximation holds only when $\overline{y(t)} \approx y_\infty$, i.e., when the average filling state of the pool is similar to the filling state at the end of an interstimulus interval. This is not the case for large p. However, then, $\tau_B \cdot p$ is likely to be larger than Δt for frequencies that are sufficiently high to induce significant depression. Taken together, it can be concluded that, whenever a stimulus induces significant depression, the steady-state level of synaptic transmission will be proportional to the average $[Ca^{++}]_i$ level, which, as concluded above, does not depend on the presence of buffers.

Eq. B1 also allows estimation of the extra recruitment of vesicles following a single stimulus in case the $[Ca^{++}]_i$ transient is short with respect to pool recovery at basal $[Ca^{++}]_i$. We choose t_1 to represent the time of the stimulus and t_2 some time later when the $[Ca^{++}]_i$ transient has subsided, but obeying the condition $t_2 - t_1 \ll \tau_B$. Then, the second term in Eq. B1 is small with respect to the first one (for $\overline{x(t)} > x_b$) and the increment in n_B will again be given by the $[Ca^{++}]_i$ integral, i.e., it will not depend on the presence of buffers.

This work was supported by a grant from the Deutsche Forschungsgemeinschaft (SFB 406).

REFERENCES

Atluri, P. P., and W. G. Regehr. 1996. Determinants of the time course of facilitation at the granule cell to purkinje cell synapse. *J. Neurosci.* 16:5661–5671.

Betz, W. J. 1970. Depression of transmitter release at the neuromuscular junction of the frog. *J. Physiol.* 206:629–644.

Borst, J. G. G., F. Helmchen, and B. Sakmann. 1995. Pre- and postsynaptic whole-cell recordings in the medial nucleus of the trapezoid body of the rat. *J. Physiol.* 489:825–840.

Borst, J. G. G., and B. Sakmann. 1996. Calcium influx and transmitter release in a fast CNS synapse. *Nature.* 383:431–434.

Borst, J. G. G., and B. Sakmann. 1999. Effect of changes in action potential shape on calcium currents and transmitter release in a calyx-type synapse of the rat auditory brainstem. *Phil. Trans. R. Soc. Lond. B.* 354: 355–363.

Bronstein, I. N., and K. A. Semendjajew. 1991. Taschenbuch der Mathematik. Teubner Verlagsgesellschaft, Stuttgart, Leipzig, Germany.

Chad, J. E., and R. Eckert. 1984. Calcium domains associated with individual channels can account for anomalous voltage relations of Ca-dependent responses. *Biophys. J.* 45:993–999.

Charlton, M. P., S. J. Smith, and R. S. Zucker. 1982. Role of presynaptic calcium ions and channels in synaptic facilitation and depression at the squid giant synapse. *J. Physiol.* 323:173–193.

Delaney, K. R., and D. W. Tank. 1994. A quantitative measurement of the dependence of short-term synaptic enhancement on presynaptic residual calcium. *J. Neurosci.* 14:5885–5902.

Dittman, J. S., and W. G. Regehr. 1998. Calcium-dependence and recovery kinetics of presynaptic depression at the climbing fiber to Purkinje cell synapse. *J. Neurosci.* 18:6147–6162.

Elmquist, D., and D. M. J. Quastel. 1965. A quantitative study of end-plate potentials in isolated human muscle. *J. Physiol.* 178:505–529.

Fisher, S. A., T. M. Fischer, and T. J. Carew. 1997. Multiple overlapping processes underlying short-term synaptic enhancement. *TINS.* 20: 170–177.

Forsythe, I. D. 1994. Direct patch recording from identified presynaptic terminals mediating glutamatergic EPSCs in the rat CNS, in vitro. *J. Physiol.* 479:381–387.

Gingrich, K. J., and J. H. Byrne. 1985. Simulation of synaptic depression, posttetanic potentiation, and presynaptic facilitation of synaptic potentials from sensory neurons mediating Gill-withdrawal reflex in Aplysia. *J. Neurophys.* 53:652–669.

Grynkiewicz, G., M. Poenie, and R. Tsien. 1985. A new generation of Ca^{2+} indicators with greatly improved fluorescence properties. *J. Biol. Chem.* 260:3440–3450.

Heidelberger, R., C. Heinemann, E. Neher, and G. Matthews. 1994. Calcium dependence of the rate of exocytosis in a synaptic terminal. *Nature.* 371:513–515.

Heinemann, C., L. v. Rüden, R. H. Chow, and E. Neher. 1993. A two-step model of secretion control in neuroendocrine cells. *Pflügers Arch.* 424: 105–112.

Helmchen, F., J. G. G. Borst, and B. Sakmann. 1997. Calcium dynamics associated with a single action potential in a CNS presynaptic terminal. *Biophys. J.* 72:1458–1471.

Kamiya, H., and R. S. Zucker. 1994. Residual Ca^{2+} and short-term synaptic plasticity. *Nature.* 371:603–606.

Katz, B., and R. Miledi. 1968. The role of calcium in neuromuscular facilitation. *J. Physiol.* 195:481–492.

Kusano, K., and E. M. Landau. 1975. Depression and recovery of transmission at the squid giant synapse. *J. Physiol.* 245:13–31.

Liley, A. W., and K. A. K. North. 1953. An electrical investigation of effects of repetitive stimulation on mammalian neuromuscular junction. *J. Neurophys.* 16:509–527.

Llinás, R., M. Sugimori, and S. M. Simon. 1982. Transmission by presynaptic spike-like depolarization in the squid giant synapse. *Proc. Natl. Acad. Sci. USA.* 79:2415–2419.

Llinás, R., M. Sugimori, and R. B. Silver. 1995. The concept of calcium concentration microdomains in synaptic transmission. *Neuropharmacology.* 34:1443–1451.

Naraghi, M., and E. Neher. 1997. Linearized buffered Ca^{2+} diffusion in microdomains and its implications for calculation of $[Ca^{2+}]$ at the mouth of a calcium channel. *J. Neurosci.* 17:6961–6973.

Neher, E., and G. J. Augustine. 1992. Calcium gradients and buffers in bovine chromaffin cells. *J. Physiol.* 450:273–301.

Neher, E. 1998a. Vesicle pools and Ca^{2+}-microdomains: new tools for understanding their roles in neurotransmitter release. *Neuron.* 20: 389–399.

Neher, E. 1998b. Usefulness and limitations of linear approximations to the understanding of Ca^{++} signals. *Cell Calcium.* 24:345–357.

Quastel, D. M. J. 1997. The binomial model in fluctuation analysis of quantal neurotransmitter release. *Biophys. J.* 72:728–753.

Rahamimoff, R. 1968. A dual effect of calcium ions on neuromuscular facilitation. *J. Physiol.* 195:471–480.

Regehr W. G., K. D. Delaney, and D. W. Tank. 1994. The role of presynaptic calcium in short-term enhancement at the hippocampal mossy fiber synapse. *J. Neurosci.* 14:523–537.

Roberts, W. M. 1994. Localization of calcium signals by a mobile calcium buffer in frog saccular hair cells. *J. Neurosci.* 14:3246–3262.

Schneggenburger, R., A. C. Meyer, and E. Neher. 1999. Released fraction and total size of a pool of immediately available transmitter quanta at a calyx synapse. *Neuron.* 23:399–409.

Simon, S. M., and R. R. Llinás. 1985. Compartmentalization of the submembrane calcium activity during calcium influx and its significance in transmitter release. *Biophys. J.* 48:485–498.

Smith, C., T. Moser, T. Xu, and E. Neher. 1998. Cytosolic Ca^{2+} acts by two separate pathways to modulate the supply of release-competent vesicles in chromaffin cells. *Neuron.* 20:1243–1253.

Stevens, C. F., and J. F. Wesseling. 1998. Activity-dependent modulation of the rate at which synaptic vesicles become available to undergo exocytosis. *Neuron.* 21:415–424.

Swandulla, D., M. Hans, K. Zipser, G. J. Augustine. 1991. Role of residual calcium in synaptic depression and posttetanic potentiation: fast and slow calcium signaling in nerve terminals. *Neuron.* 7:915–926.

Tsodyks, M. V., and H. Markram. 1997. The neural code between neocortical pyramidal neurons depends on neurotransmitter release probability. *Proc. Natl. Acad. Sci. USA.* 94:719–723.

Vere-Jones, D. 1966. Simple stochastic models for the release of quanta of transmitter from a nerve terminal. *Aust. J. Statist.* 8:53–63.

v. Gersdorff, H., R. Schneggenburger, S. Weis, and E. Neher. 1997. Presynaptic depression at a calyx synapse: the small contribution of metabotropic glutamate receptors. *J. Neurosci.* 17:8137–8146.

Wang, L. Y., and L. K. Kaczmarek. 1998. High-frequency firing helps replenish the readily releasable pool of synaptic vesicles. *Nature.* 394: 384–388.

Weis, S. 1998. Mechanismen der Kurzzeitplastizität an neuronalen Synapsen. Ph.D. thesis, University of Göttingen, Germany.

Wu, L. G., and J. G. G. Borst. 1999. The reduced release probability of releasable vesicles during recovery from short-term synaptic depression. *Neuron*. (In press).

Worden, M. K., M. Bykhovskaia, and J. T. Hackett. 1997. Facilitation at the lobster neuromuscular junction: a stimulus-dependent mobilization model. *J. Neurophys.* 78:417–428.

Yamada, W. M., and R. S. Zucker. 1992. Time course of transmitter release calculated from simulations of a calcium diffusion model. *Biophys. J.* 61:671–682.

Zucker, R. S. 1974. Characteristics of crayfish neuromuscular facilitation and their calcium dependence. *J. Physiol.* 241:91–110.

Zucker, R. S. 1996. Exocytosis: A molecular and physiological perspective. *Neuron.* 17:1049–1055.

Zucker, R. S. 1999. Calcium- and activity-dependent synaptic plasticity. *Curr. Op. Neurobiol.* 9:305–313.